12-2014

Oral Delivery of ACE2/Ang-(1–7) Bioencapsulated in Plant Cells Protects Against Experimental Uveitis and Autoimmune Uveoretinitis

Pollob K. Shil

Kwang-Chul Kwon
University of Pennsylvania

Ping Zhu

Amrisha Verma

Henry Daniell
University of Pennsylvania

See next page for additional authors

Recommended Citation

Shil, P. K., Kwon, K., Zhu, P., Verma, A., Daniell, H., & Li, Q. (2014). Oral Delivery of ACE2/Ang-(1–7) Bioencapsulated in Plant Cells Protects Against Experimental Uveitis and Autoimmune Uveoretinitis. *Molecular Therapy, 22* (12), 2069-2082. http://dx.doi.org/10.1038/mt.2014.179

Oral Delivery of ACE2/Ang-(1–7) Bioencapsulated in Plant Cells Protects Against Experimental Uveitis and Autoimmune Uveoretinitis

Abstract

Hyperactivity of the renin-angiotensin system (RAS) resulting in elevated Angiotensin II (Ang II) contributes to all stages of inflammatory responses including ocular inflammation. The discovery of angiotensin-converting enzyme 2 (ACE2) has established a protective axis of RAS involving ACE2/Ang-(1–7)/Mas that counteracts the proinflammatory and hypertrophic effects of the deleterious ACE/AngII/AT1R axis. Here we investigated the hypothesis that enhancing the systemic and local activity of the protective axis of the RAS by oral delivery of ACE2 and Ang-(1–7) bioencapsulated in plant cells would confer protection against ocular inflammation. Both *ACE2* and *Ang-(1–7)*, fused with the non-toxic cholera toxin subunit B (*CTB*) were expressed in plant chloroplasts. Increased levels of ACE2 and Ang-(1–7) were observed in circulation and retina after oral administration of CTB-ACE2 and Ang-(1–7) expressing plant cells. Oral feeding of mice with bioencapsulated ACE2/Ang-(1–7) significantly reduced endotoxin-induced uveitis (EIU) in mice. Treatment with bioencapsulated ACE2/Ang-(1–7) also dramatically decreased cellular infiltration, retinal vasculitis, damage and folding in experimental autoimmune uveoretinitis (EAU). Thus, enhancing the protective axis of RAS by oral delivery of ACE2/Ang-(1–7) bioencapsulated in plant cells provide an innovative, highly efficient and cost-effective therapeutic strategy for ocular inflammatory diseases.

Disciplines

Dentistry

Author(s)

Pollob K. Shil, Kwang-Chul Kwon, Ping Zhu, Amrisha Verma, Henry Daniell, and Qiuhong Li

Oral Delivery of ACE2/Ang-(1–7) Bioencapsulated in Plant Cells Protects against Experimental Uveitis and Autoimmune Uveoretinitis

Pollob K Shil[1], Kwang-Chul Kwon[2], Ping Zhu[1], Amrisha Verma[1], Henry Daniell[2] and Qiuhong Li[1]

[1]Department of Ophthalmology, College of Medicine, University of Florida, Gainesville, Florida, USA; [2]Department of Biochemistry, School of Dental Medicine, University of Pennsylvania, Philadelphia, Pennsylvania, USA;

Hyperactivity of the renin-angiotensin system (RAS) resulting in elevated Angiotensin II (Ang II) contributes to all stages of inflammatory responses including ocular inflammation. The discovery of angiotensin-converting enzyme 2 (ACE2) has established a protective axis of RAS involving ACE2/Ang-(1–7)/Mas that counteracts the pro-inflammatory and hypertrophic effects of the deleterious ACE/AngII/AT1R axis. Here we investigated the hypothesis that enhancing the systemic and local activity of the protective axis of the RAS by oral delivery of ACE2 and Ang-(1–7) bioencapsulated in plant cells would confer protection against ocular inflammation. Both *ACE2* and *Ang-(1–7)*, fused with the non-toxic cholera toxin subunit B (*CTB*) were expressed in plant chloroplasts. Increased levels of ACE2 and Ang-(1–7) were observed in circulation and retina after oral administration of CTB-ACE2 and Ang-(1–7) expressing plant cells. Oral feeding of mice with bioencapsulated ACE2/Ang-(1–7) significantly reduced endotoxin-induced uveitis (EIU) in mice. Treatment with bioencapsulated ACE2/Ang-(1–7) also dramatically decreased cellular infiltration, retinal vasculitis, damage and folding in experimental autoimmune uveoretinitis (EAU). Thus, enhancing the protective axis of RAS by oral delivery of ACE2/Ang-(1–7) bioencapsulated in plant cells provide an innovative, highly efficient and cost-effective therapeutic strategy for ocular inflammatory diseases.

Received 28 April 2014; accepted 9 September 2014; advance online publication 14 October 2014. doi:10.1038/mt.2014.179

INTRODUCTION

Retinal inflammation is one of the major causes of visual impairment and is also a key underlying factor for a range of retinal diseases. Uveitis is a sight threatening intraocular inflammatory disorder caused by infectious agents, autoimmune mechanisms, exposure to toxins and many other unknown factors[1] and has been estimated to account for 5–15% of all cases of total blindness in the United States.[2] Endotoxin-induced uveitis (EIU) is an animal model of acute ocular inflammation induced by the administration of lipopolysaccharide (LPS).[3] LPS enhances the expression of various inflammatory mediators resulting in the breakdown of blood-ocular barriers and infiltration of inflammatory cells in ocular tissues which contribute to the development of EIU.[3] Experimental autoimmune uveoretinitis (EAU) is an animal model of autoimmune uveitis that resembles human uveitis.[4] It is an organ specific, T-cell mediated autoimmune disease that targets the neural retina and related tissues. Immunization of rodents with retinal antigen such as interphotoreceptor retinoid binding protein (IRBP) to induce EAU is a widely used experimental model to investigate the immunopathogenesis of autoimmune uveitis.[4] The clinical, biochemical, immunological and histological characteristics make EIU and EAU suitable *in vivo* models to evaluate the efficacy of therapeutics for the treatment of inflammatory ocular diseases in humans.[3,4]

The renin-angiotensin system (RAS) plays an important role not only in the cardiovascular homeostasis, but also in the pathogenesis of inflammation and autoimmune dysfunction in which Angiotensin II (Ang II) functions as the potent proinflammatory effector via Angiotensin Type 1 receptor (AT1 receptor). Most components of RAS have been identified in every organ including the eye. The tissue-specific RAS is believed to exert diverse physiological effects locally independent of circulating Ang II.[5] Discovery of angiotensin-converting enzyme 2 (ACE2) has resulted in the establishment of a novel axis of RAS involving ACE2/Ang-(1–7)/Mas.[6] ACE2 is a zinc-metallopeptidase able to cleave Ang II to form Angiotensin-(1–7) [Ang-(1–7)]. Ang-(1–7), a biologically active peptide, binds to a G-protein coupled receptor, Mas, and activates signaling pathways that counteract the effects of Ang II.[6] Thus, the ACE2/Ang-(1–7)/Mas axis has emerged as a critical regulator of Ang II/AT1R signaling. Several studies have shown that ACE2/Ang-(1–7)/Mas axis also influences inflammatory responses and negatively modulates leukocyte migration, cytokine expression and release, and fibrogenic pathways.[7] We have recently shown that increased expression of ACE2 and Ang-(1–7) reduced diabetes-induced retinopathy and inflammation in both mouse and rat models of diabetic retinopathy,[8] activation of endogenous ACE2 activity reduced endotoxin-induced uveitis,[9] providing the proof-of-concept that enhancing the protective axis of RAS is a promising therapeutic strategy for ocular inflammatory diseases.

However, the ability to deliver drugs efficiently to the retina or the brain remains a key challenge due to anatomic barriers

Correspondence: Qiuhong Li, Department of Ophthalmology, University of Florida, Gainesville, Florida 32610-0284, USA. E-mail: qli@ufl.edu or Henry Daniell, Director of Translational Research, University of Pennsylvania, 240 South 40th Street, 547 Levy Building, Philadelphia, Pennsylvania 19104-6030, USA. E-mail: hdaniell@upenn.edu

and physiological clearance mechanisms.[10] Plant chloroplast genetic engineering system to express therapeutic proteins is emerging as a highly efficient, cost-effective approach for therapeutic interventions of many pathologic conditions.[11] In contrast to current protein production systems (mammalian, yeast, or bacteria), the transplastomic system requires no complex production/purification steps.[11] Current biopharmaceuticals are not affordable to more than half of the global population because of use of prohibitively expensive production, purification and delivery systems.[11] However, chloroplasts produce the same biopharmaceuticals at a significantly lower cost by eliminating fermentation, purification, cold chain and sterile delivery systems. Such cGMP facilities to produce plants for human clinical studies are already in use in the US (*e.g.*, Fraunhofer, Delaware, Kentucky Bioprocessing, etc.). Ultimately, the therapeutic proteins will be provided to patients as capsules after lyophilization of plant cells, facilitating prolonged storage at room temperature. In addition, bioencapsulation of therapeutic proteins within plant cell walls enable oral delivery by their protection in the digestive system.[11,12] The bioencapsulated proteins that pass through the stomach are released in the intestine with the aid of commensal bacteria.[13,14] Bacteria inhabiting the human gut have evolved to utilize complex carbohydrates in plant cell wall and are capable of utilizing almost all of plant glycans. So the gut microbes recognize, import, and digest plant cell wall consisting of cellulose, hemicellulose, and pectin. Up to 10% daily energy is obtained from polysaccharide fiber via the symbiotic bacteria living in human gut. These polysaccharides are broken down to sugars and fermented to short fatty acids then absorbed by human gut. Therapeutic proteins enter circulation by receptor monosialotetrahexosylganglioside (GM1) mediated delivery when fused with the non-toxic subunit B of cholera toxin (CTB) as the transmucosal carrier.[11,15–19] The use of CTB as a transmucosal carrier can facilitate the transportation of conjugated proteins into circulation through its strong binding to GM1 because large mucosal area of human intestine (~1.8–2.7 m^2 (ref. [20]) facilitates CTB to bind an intestinal epithelium cell up to a maximum of 15,000 CTB.[21] Furthermore, the GM1 gangliosides receptors are also found in the plasma membranes of most cells, particularly most abundant in the nervous system and retina,[22] allowing efficient uptake of CTB fusion protein in the brain and retinal cells as observed in our recent study.[23]

Considering the proven anti-inflammatory actions of ACE2 and Ang-(1–7) and the ability of CTB to cross the epithelial barrier and facilitate neuronal uptake, we hypothesized that oral delivery of ACE2 and Ang-(1–7) fused with CTB bioencapsulated in plant cells will enhance both systemic and local activity of the protective axis of RAS and confer protection against ocular inflammation. In this study, we tested this hypothesis in two mouse models of ocular inflammation. We observed that oral administration of CTB-ACE2 and CTB-Ang-(1–7) bioencapsulated in plant cells reduced ocular inflammation in both EIU and EAU models, providing proof-of-concept that enhancing the protective axis of RAS by oral delivery of ACE2/Ang-(1–7) bioencapsulated in plant cells provides an innovative, highly efficient and cost-effective therapeutic strategy for ocular inflammation such as uveitis and autoimmuneuveoretinitis.

RESULTS

Creation of transplastomic plants expressing CTB-ACE2 and CTB-Ang-(1–7)

The CTB-fused therapeutic genes were cloned into the chloroplast transformation vector, pLD. The hinge site (**Figure 1a**) was introduced between CTB and therapeutic proteins to avoid steric hindrance so as to facilitate proper formation of pentameric structure of CTB fused to therapeutics when expressed in chloroplasts. Since the pentamer structure of CTB plays critical role in translocating fusion proteins into epithelial cell via GM1 receptor, the introduction of hinge is required to facilitate to form proper structure of the CTB fusion proteins. Furin cleavage site (**Figure 1a**) is responsible for the release of therapeutic proteins from CTB after internalization into cells. The furin is ubiquitously present in the body and the consensus cleavage site is well characterized.[24] The introduction of the consensus furin cleavage site between CTB and the proteins will ensure efficient release of the therapeutic proteins from CTB in the circulation. For the site-specific integration of the *CTB-ACE2/-Ang-(1–7)* expression cassette into chloroplast genome, the cassette was flanked by *trnI* and *trnA* sequence, which are homologous to endogenous chloroplast sequence. Light regulated strong chloroplast promoter, *PsbA*, was used to express the fusion gene. To screen chloroplast transformants, aminoglycoside 3′-adenylyltransferase gene (*aadA*) was driven under the control of ribosomal *rRNA* promoter (*Prrn*) to disarm the inhibitory action of spectinomycin on chloroplast translation (**Figure 1a**). The sequence-confirmed chloroplast transformation vector was bombarded onto leaf disc to create the transplastomic plants expressing *CTB-ACE2* and *CTB-Ang-(1–7)*, using biolistic particle delivery system. Shoots emerged from spectinomycin containing regeneration medium were investigated for the site specific integration of the expression cassette into chloroplast genome, using PCR analysis. The specific primer sets were designed to amplify fragments in the size of ~1.65 kb with 3P/3M for both *CTB-ACE2* and *CTB-Ang-(1–7)*, ~4.5 and ~2.2 kb with 5P/2M for *CTB-ACE2* and *CTB-Ang-(1–7)*, respectively, and ~3.0 and ~1.1 kb with 5P/R for *CTB-ACE2* and *CTB-Ang-(1–7)*, respectively. As seen in the **Figure 1b**,**c**, the positive shoots displaying the expected right size fragments were subjected to two more rounds of tissue culture under the antibiotic pressure to achieve homoplasmy. The homoplasmic plants were confirmed by Southern blot analysis (data not shown), transferred and grown in a temperature- and humidity-controlled greenhouse. The expression level of CTB-fused therapeutic proteins of mature leaves was measured quantitatively using densitometry and Image J or ELISA with known amount of CTB proteins to generate standard curve. The level was up to 2.14% and 8.7% of total leaf protein for CTB-ACE2 and CTB-Ang-(1–7) at their peak, respectively (data not shown). For consistency of batches between harvests, the leaf harvests were always done at evening time around 6 pm to maximize accumulation of the fusion proteins expressed under the control of light regulated promoter, *psbA* which can stay activated during the daylight. Also, only mature leaves were chosen for harvest to maintain similar expression levels of the proteins between batches. While it is difficult to precisely control expression levels at the time of harvest, dosage is precisely determined after lyophilization and

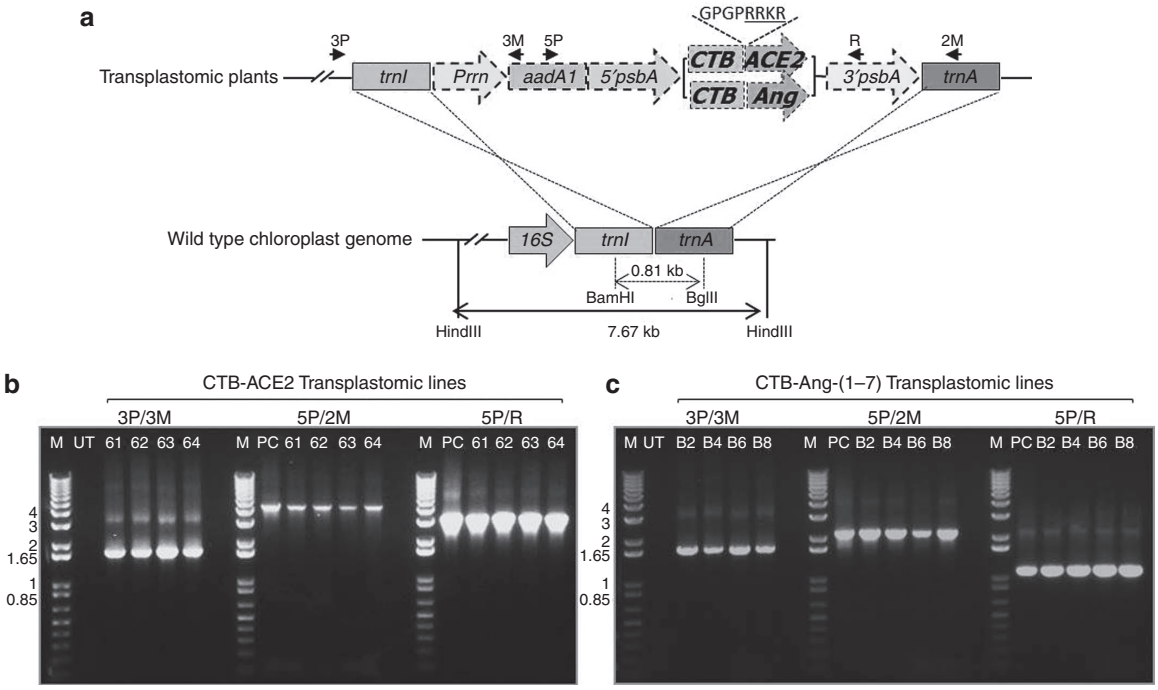

Figure 1 Creation of transplastomic lines expressing *CTB-ACE2* and *CTB-Ang-(1–7)*. (**a**) Schematic representation of chloroplast transformation vector containing *CTB-ACE2* and *Ang-(1–7)* expression cassettes. *Prrn*, rRNA operon promoter; *aadA*, aminoglycoside 3′-adenylytransferase gene; *PpsbA*, promoter and 5′ UTR of *psbA* gene; *CTB*, coding sequence of non-toxic cholera B subunit; *ACE2* and *Ang*, coding sequence for Angiotensin-converting enzyme 2 and Angiotensin-(1–7), respectively; *TpsbA*, 3′ UTR of *psbA* gene; *trnI*, isoleucyl-tRNA; *trnA*, alanyl-tRNA; Amino acid sequence, hinge, furin cleavage site. Arrows represent primers used to amplify the site-specific integration of the expression cassette. Restriction enzymes used for Southern blot analysis were indicated as BamHI/BglII for the generation of probe and HindIII for the digestion of genomic DNA. (**b**,**c**) PCR analysis of the site specific integration of the transgenes with 3P/3M, 5P/2M, and 5P/R primer sets. M, DNA size marker; UT, untransformed wild-type; #61–64, CTB-ACE2 transplastomic line; #B2, B4, B6, and B8, CTB-Ang-(1–7) transplastomic lines; PC, *CTB-ACE2*, and *-Ang-(1–7)* containing vector.

delivered by varying the weight of lyophilized powder in each capsule or gavage.

Characterization of CTB-fused therapeutic proteins expressed in chloroplasts

CTB was used as a carrier to allow therapeutic proteins to pass through both epithelial and blood–retinal barrier,[23] which is mediated by the interaction between pentameric CTB and GM1 receptor. To investigate the proper folding and assembly of the pentameric structure of CTB-fused therapeutic proteins in chloroplasts, western blot analysis was performed with CTB-Ang-(1–7). Proteins were extracted under non-denaturing conditions, followed by either treatment with or without denaturing agents, prior to running on SDS-acrylamide gel. There was negligible change in band patterns for oligomeric structures of CTB-Ang-(1–7) when protein was treated with DTT alone (**Figure 2a**). In contrast, boiling samples showed dramatic change in band patterns (**Figure 2a**). This is consistent with the previous studies on dissociation of CTB pentameric structure.[25] Multiple interactions between CTB monomers, such as 30 hydrogen bonds, 7 salt bridges and hydrophobic interactions, make pentameric structure of CTB highly resistant to the dissociation so the pentamer structure is not affected by denaturants such as SDS and DTT. However, the structure can be dissociated by using heat energy. This could be due to the difference in accessibility of each denaturing agents to their targets. The access of DTT to the intramolecular disulfide bond of monomer is not easy unless pentameric structure dissociates first, due to the intimate interactions between monomers described above. As expected, both denaturing agents showed no high molecular weight oligomers (pentamer-pentmer interactions), but dimeric and monomeric forms of CTB-Ang-(1–7) were observed (**Figure 2a**). The intramolecular disulfide bond of CTB monomer was easily disrupted by DTT after boiling than either boiling alone or DTT alone (**Figure 2a**). Boiling allowed easy access of DTT to the internal disulfide bond by breaking intimate interactions between CTB monomers (hydrogen bonds and salt bridges) (**Figure 2a**). From these results, it is evident that the disulfide bond of CTB-Ang-(1–7) monomer was properly formed and the interactions between the monomers of pentameric structure of CTB-Ang-(1–7) were well established in chloroplasts.

For clinical application, long-shelf life and stability of therapeutic protein expressed in plants are very important for successful and cost-effective treatment. Therefore, lyophilized CTB-fused therapeutic protein leaves were fully characterized. The weight of lyophilized leaf is usually reduced by 90–95% as a result of removal of water from plant cells, leading to more total protein per mg. Extraction of concentrated proteins from lyophilized leaf materials needs more volume of extraction buffer because the amount of water lost in the process of lyophilization is slowly reabsorbed by the dried materials. For quantitation of lyophilized leaf materials, 10 mg of lyophilized powered leaf materials were resuspended in 300 µl extraction buffer in contrast to 100 mg of fresh leaf materials in the same volume of extraction buffer. Then the extracted total proteins were used for quantification for comparison between fresh and lyophilized leaf materials. Western blot analysis for the

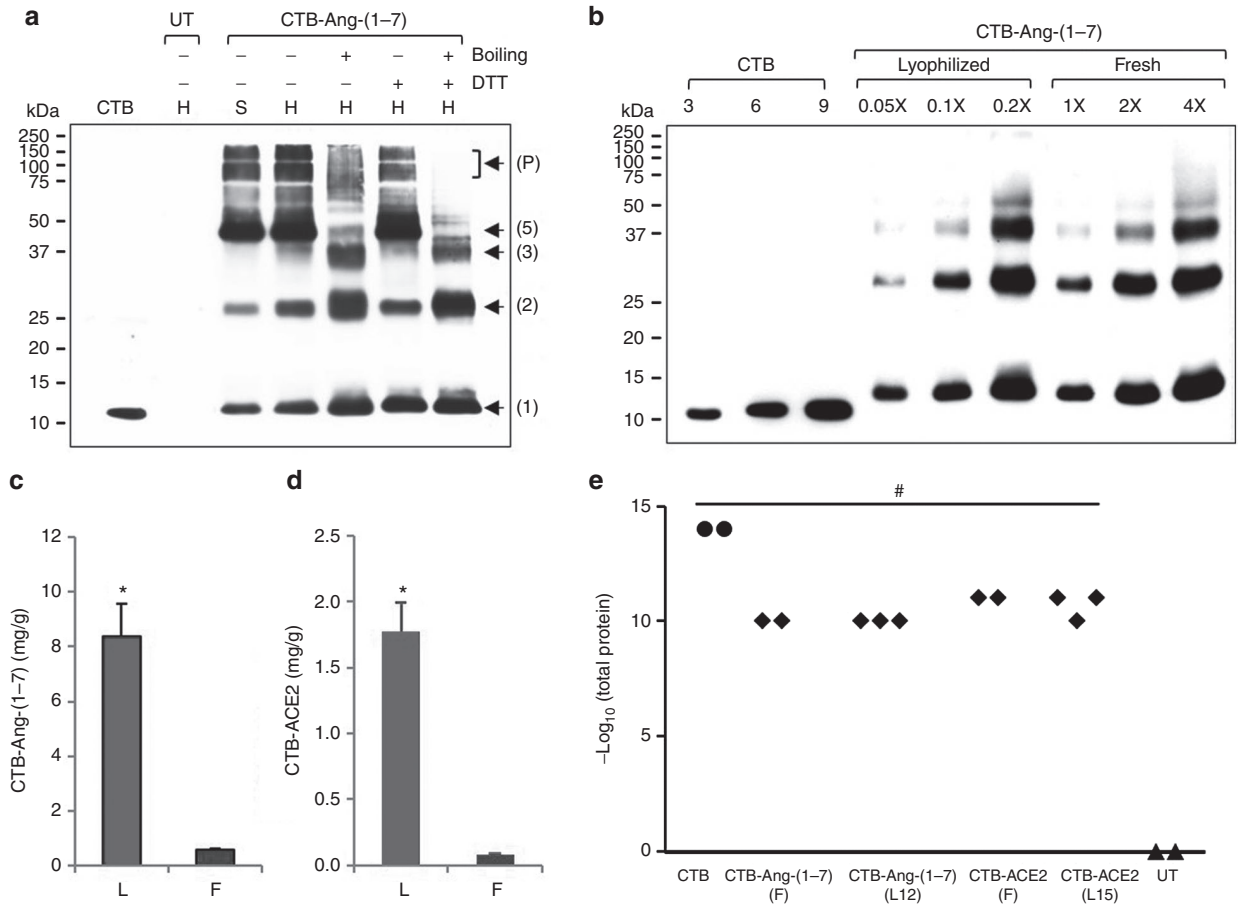

Figure 2 Evaluation of proper formation of pentameric structure and lyophilization for the CTB fusion proteins. (**a**) Western blot analysis to investigate the proper folding and assembly of CTB-Ang-(1–7) expressed in chloroplasts. Four micrograms of total leaf protein were loaded for each lane with (+) or without (–) treatment of denaturing agents. CTB, purified non-toxic cholera B subunit (10 ng); UT, untransformed wild-type; DTT, 100 mmol/l; boiling, incubation of samples in boiling water for 3 minutes; H, homogenate total leaf protein; S, supernatant fraction after centrifugation of the total leaf protein; Arrows and numbers, locations of monomer and oligomers of CTB-Ang-(1–7); P, pentamer-pentamer complexes. (**b**) Western blot analysis for the comparison of the level of CTB-Ang-(1–7) in lyophilized (L) and fresh (F) leaves. Equal amount of lyophilized and fresh leaf material (10 mg) was extracted in same volume (300 µl) of extraction buffer. 1X represents 1 µl of homogenate protein resuspended in extraction buffer. The samples were boiled in DTT prior to loading on SDS acrylamide gel. Purified CTB standard protein was loaded as indicated for densitometric analysis. (**c**,**d**) Comparison of the level of CTB-Ang-(1–7) and –ACE2 in lyophilized (L) and fresh (F) leaves. Data are means ± SD of three independent experiments. (**e**) GM1 binding assay of CTB-ACE2 and -Ang-(1–7). Extracted total protein samples were serially diluted up to 10 pg/ul, which means 11 on the Y axis, and used for GM1 binding assay. The binding affinity was read at 450 nm then an absorbance of ≥0.1 after background signal substraction was determined as positive. Two and three different batches were examined for fresh and lyophilized leaf materials, respectively, and indicated as black diamond. CTB, purified non-toxic cholera B subunit (black circle); UT, untransformed wild-type (black triangle); F, fresh; L, lyophilized; 12 and 15, 12- and 15-month storage at room temperature. *$P < 0.001$ (versus fresh); #$P < 0.001$ (versus WT).

CTB-Ang-(1–7) showed that the band patterns between fresh and 3-month-old lyophilized leaf materials were identical (**Figure 2b**), confirming stability during lyophilization and prolonged storage at room temperature. As seen in the blot, twenty-time less lyophilized protein sample loaded showed similar band intensities to fresh leaf proteins (**Figure 2b**). The quantity of CTB-Ang-(1–7) in fresh and lyophilized leaves was measured using immunoblots (**Figure 2b**) and Image J software. The quantity of lyophilized CTB-Ang-(1–7) increased 14.3 times in lyophilized leaves when compared to fresh leaves (**Figure 2c**). The lyophilized CTB-ACE2 leaves showed 20.5-fold more CTB-ACE2 than fresh leaves when quantified using ELISA (**Figure 2d**).

In this study, we observed that there was no damage or loss of the fusion protein (**Figure 2b**) under the optimized lyophilization conditions. Moreover, the intactness of the pentameric structure of the lyophilized CTB-fused proteins was well preserved up to 15 months at room temperature, as confirmed in GM1 binding assay which showed binding affinity of the lyophilized CTB-fused proteins to GM1 as compared to respective positive control, CTB (**Figure 2e**). Taken together, the homoplasmic transplastomic plants expressing CTB-ACE2 and -Ang-(1–7) were created and the fusion protein was properly expressed, folded, and assembled in chloroplasts. The folding, assembly and functionality of therapeutic proteins were well preserved in lyophilized leaves.

ACE2 activity assay using protein extracts isolated from plant leaves showed that plant cell expressed human ACE2 is enzymatically active (**Figure 3a**). To investigate the *in vivo* potential of CTB-ACE2 and CTB-Ang-(1–7) to cross the intestinal barrier and tissue uptake, wild-type (WT) C57Bl/6J mice were fed with either fresh (F, ~500 mg/mouse), or tenfold less lyophilized (L,

~50 mg/mouse) CTB-ACE2, or control untransformed (WT) leaf materials for three days, mice were sacrificed at 5 hours after the last gavage. Circulatory and retinal ACE2 and Ang-(1–7) levels were measured by ACE2 activity assay, EIA and Western blotting (**Figure 3**). ACE2 protein can be detected in both serum and retina 5 hours after oral gavage (**Figure 3b**). Oral administration of either fresh frozen (F) or lyophilized (L) CTB-ACE2 transplastomic leaf materials resulted in an increase of ~40 and >20% in ACE2 enzymatic activity in serum and retina respectively when compared to WT leaf fed mice (**Figure 3c**). There was a 15% increase in plasma and nearly 50% increase in Ang-(1–7) peptide level in the retina in CTB-Ang-(1–7) expressed leaf material fed group, detected by Ang-(1–7) specific EIA kit (**Figure 3d**).

Oral administration of bioencapsulated CTB-ACE2 and CTB-Ang-(1–7) reduced the infiltration of inflammatory cells induced by EIU

We next examined the effects of ACE2 and Ang-(1–7) on endotoxin-induced infiltration of inflammatory cells such as leucocytes and monocytes in the iris, ciliary body, anterior chamber, and posterior chamber of the eye. Sagittal sections were stained with H&E and examined under bright field microscope. The histological evaluation of LPS injected eyes from mice fed with WT leaf revealed severe signs of uveitis with massive infiltration of inflammatory cells into the iris and ciliary body (ICB) (140 ± 21 cells/section), anterior chamber (265 ± 52 cells/section) and the posterior chamber (202 ± 37 cells/section) (**Figure 4**). Prophylactic treatment with CTB-ACE2 showed significantly diminished uveitis and reduced number of inflammatory cells into the ICB (60 ± 09 cells/section), anterior chamber (96 ± 15 cells/section) and also into the posterior chamber (82 ± 15 cells/section). Similar results were observed in ICB (70 ± 15 cells/section), anterior chamber (114 ± 36 cells/section) and the posterior chamber (28 ± 15 cells/section) when animals pretreated with CTB-Ang-(1–7) expressed leaf material (**Figure 4**).

The therapeutic effect of different doses of CTB-ACE2 in EIU was evaluated using lyophilized leaf materials (**Supplementary Materials and Methods**). Oral feeding of lyophilized CTB-ACE2 at 50 mg/day significantly prevented inflammatory cell infiltration

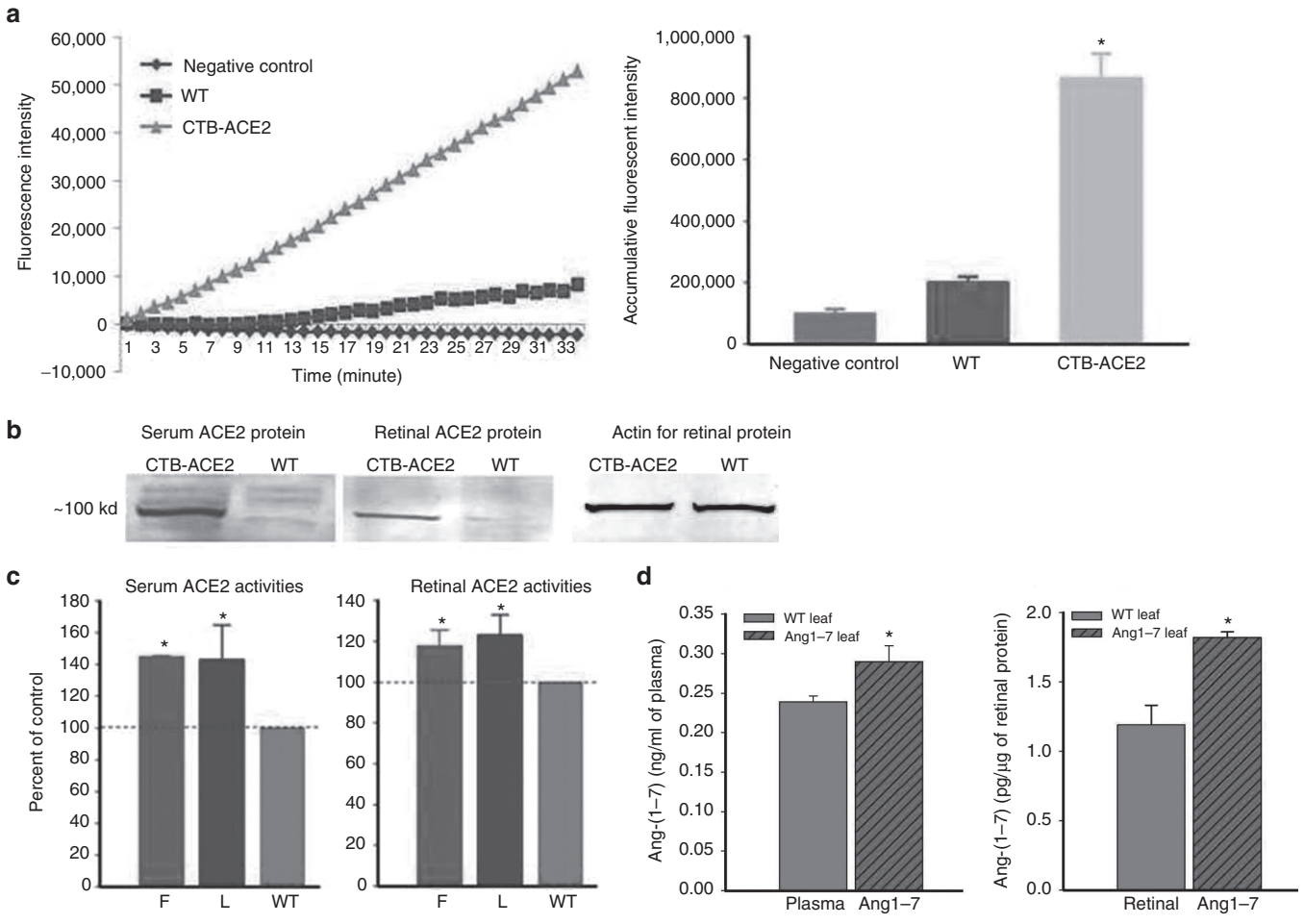

Figure 3 Characterization of plant cell expressed ACE2 activity and Ang-(1-7) levels *in vitro* and *in vivo*. (**a**) ACE2 activity assay using protein samples extracted from CTB-ACE2 transplastomic and untransformed leaf materials (WT). Assay buffer containing the substrate was also used as a negative control. (**b**) Increased ACE2 in both serum and retina in mice fed with CTB-ACE2 leaf material detected by Western blotting using an anti-ACE2 polyclonal antibody. (**c**) ACE2 activities in serum and retina from mice fed with either fresh (F, 500 mg/ mouse), or lyophilized (L, 50 mg/ mouse) CTB-ACE2 leaf materials, compared to mice fed with wild-type (WT) leaf materials; (n = 5 per group). (**d**) Ang-(1-7) levels in plasma and retinal samples in mice fed with WT and CTB-Ang-(1-7) leaf materials measured by EIA (n = 5 per group). The experiment was repeated at least twice with similar results.*P < 0.05 (versus WT leaf).

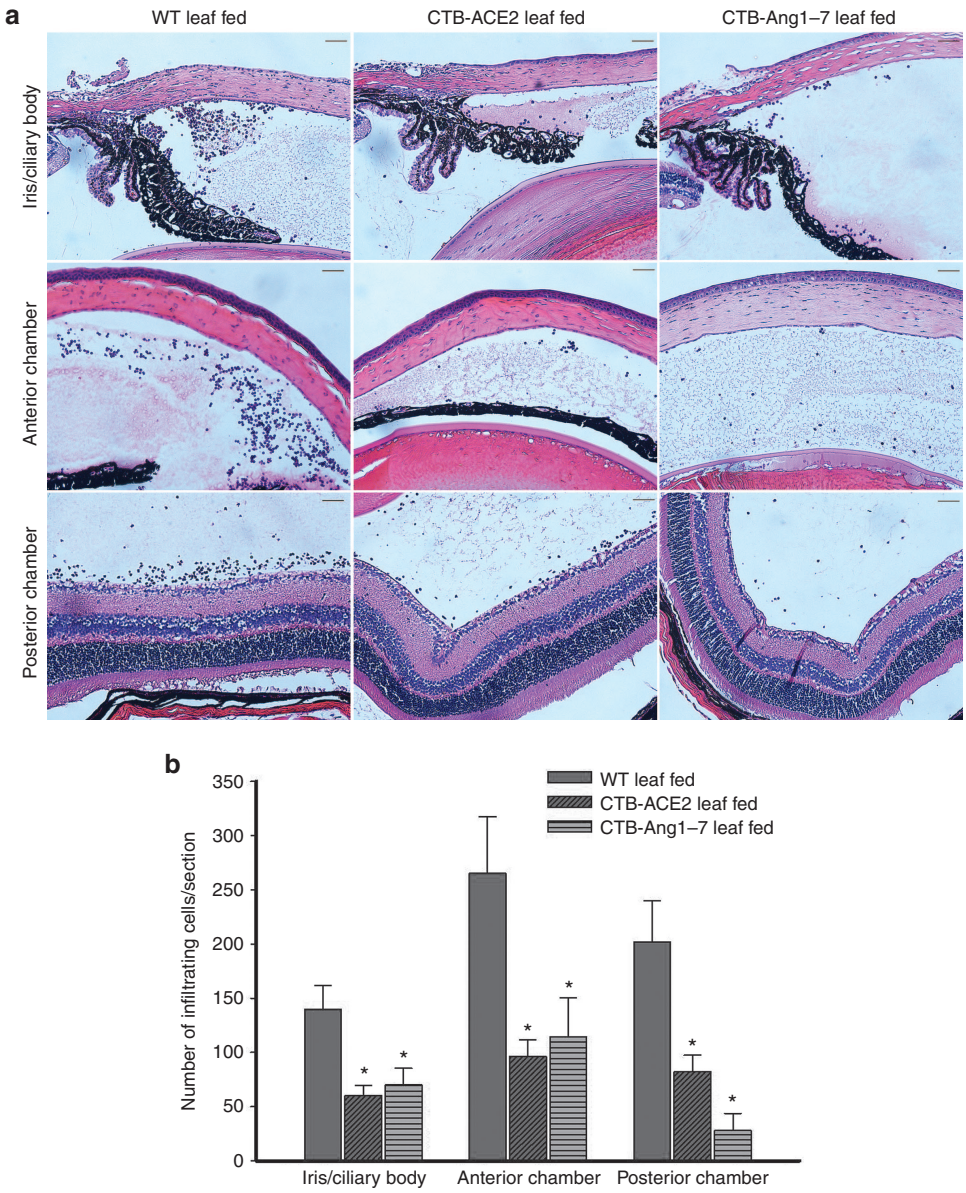

Figure 4 Histological evaluation of EIU mice. The mice were orally administered with wild-type, CTB-ACE2 and CTB-Ang-(1–7) expressed leaf material for five days before LPS (25 ng/eye) injection. Eyes were enucleated 24 hours after LPS injection, fixed and processed for paraffin sections and stained with H&E. (**a**) Representative photographs of the iris ciliary body, anterior chamber and posterior chamber. Original magnifications 20×. Bar = 50 µm. (**b**) Histopathologic score evaluation. Inflammatory cells per section in the iris ciliary body, anterior chamber and posterior chamber were counted from H&E stained paraffin sections from eyes at 24 hours after EIU induction. Values on *y*-axis represent no. of infiltrating inflammatory cells/section. Results are given as mean + SD; (n = 6 per group); *P < 0.05 (versus WT+LPS group).

into the iris and ciliary body, anterior chamber and posterior chamber to the same extent as the fresh leaf material at 500 mg/day; CTB-ACE2 feeding at 25 mg/day had moderate but significant protection, whereas 12.5 mg/day did not show any protective effect in EIU (**Supplementary Figure S1**).

Oral administration of bioencapsulated CTB-ACE2 and CTB-Ang-(1–7) reduced the expression of the inflammatory cytokinesin EIU eyes

To investigate the effects of ACE2 and Ang-(1–7) on the expression of inflammatory cytokines in EIU eyes, the mRNA levels of cytokine genes were determined by real-time RT-PCR. In the WT leaf fed mice, LPS caused a significant increase in mRNA levels of Interleukin-6 (IL-6), Interleukin-1β (IL-1β), Tumor necrosis factor-α (TNF-α) and vascular endothelial growth factor (VEGF) and this increase was reduced in mice fed with ACE2/Ang-(1–7) leaf materials (**Figure 5a**). These results suggest that ACE2 and Ang-(1–7) reduced infiltration of inflammatory cells and cytokine production through suppressing their gene expressions during EIU. To investigate the molecular mechanisms of leucocyte recruitment, the mRNA levels of intercellular adhesion molecule-1 (ICAM-1) and monocyte chemoattractant protein (MCP-1) were measured in EIU eyes. The expression of both ICAM-1 and MCP-1 was significantly increased in LPS induced EIU eyes in mice treated with WT leaf material and was significantly reduced in mice fed with CTB-ACE2 or CTB-Ang-(1–7) (**Figure 5a**).

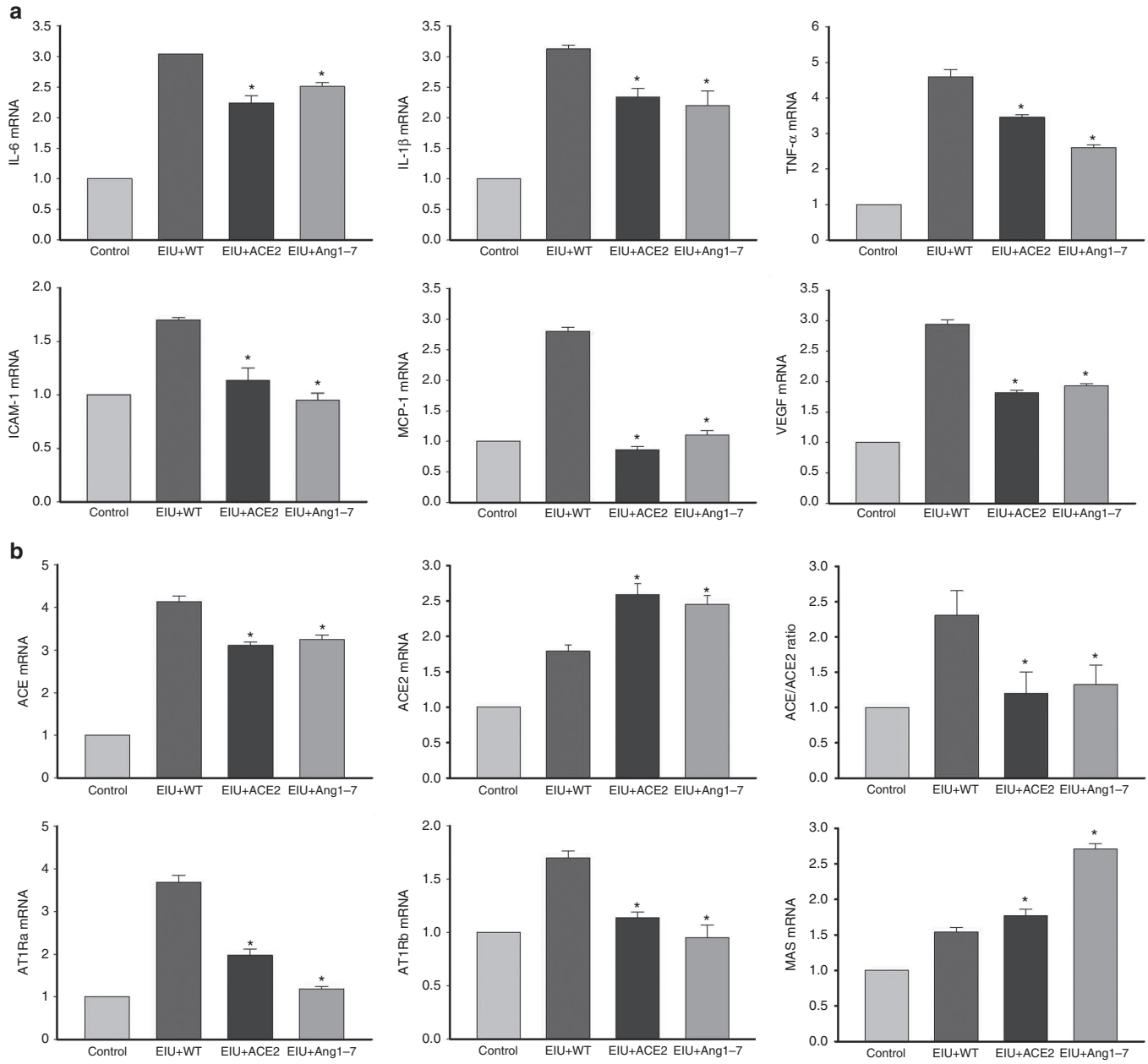

Figure 5 Real-time reverse transcriptase (RT)-PCR analysis of ocular mRNA levels of (a) inflammatory cytokines and (b) RAS genes. Values on y-axis represent fold difference compared to age-matched wild-type control ocular samples for each gene. WT ctrl, non-fed wild-type control; WT+LPS, WT leaf fed & LPS injected; ACE2+LPS, CTB-ACE2 expressed leaf fed & LPS injected; Ang-(1–7)+LPS, CTB-Ang-(1–7) expressed leaf fed & LPS injected. Data expressed as mean + SD; (n = 4 per group); *P < 0.05 (versus WT+LPS group).

The impact of oral administration of bioencapsulated CTB-ACE2 and CTB-Ang-(1–7) on the expression of the retinal RAS genes during EIU

In addition to circulating RAS, all components of RAS have been detected in the retina and a local retina RAS may play an important role in modulating local immune responses.[8,9,26] We compared ocular mRNA levels of the key RAS genes in animals fed with ACE2 and Ang-(1–7) expressing leaf materials as well as untransformed WT leaf materials. LPS-induced EIU resulted in increased expression of both ACE and ACE2, however prominent increase in ACE (more than fourfold increase) than ACE2 (less than twofold increase), resulted in increased ratio of ACE/ACE2 (**Figure 5b**). CTB-ACE2 or CTB-Ang-(1–7) oral feeding normalized the shift of ACE/ACE2 ratio (**Figure 5b**). The mRNA levels for receptors for Ang II (AT1Ra, AT1Rb) were also increased in EIU mice fed with control leaf material (~4-fold and 1.7-fold respectively) (**Figure 5b**), both of which were significantly decreased in mice fed with CTB-ACE2 or CTB-Ang (1–7). There was a slight but significant increase in Mas, the receptor for Ang-(1–7). Interestingly the Mas mRNA level in the retina was further increased in mice fed with CTB-ACE2 (approximately twofold increase), and even more increase in mice fed with CTB-Ang-(1–7) leaf material (approximately threefold increase) (**Figure 5b**), suggesting a possible feed-forward regulatory response in local retinal RAS.

Oral delivery of bioencapsulated CTB-ACE2 and CTB-Ang-(1–7) attenuated autoantigen induced uveoretinitis

Experimental autoimmune uveoretinitis was induced in an autoimmune susceptible B10.RIII mouse strain by active immunization using a peptide derived from the retinal protein IRBP.[27] Evident inflammatory reactions such as mild to severe vasculitis, focal lesions, large confluent lesions, retinal hemorrhages and folding, corneal edema etc., were observed in WT leaf fed animals by fundoscopy examination at day 14 of EAU induction (**Figure 6a**, **i**,ii). However, mice fed with CTB-ACE2 or -Ang-(1–7) leaf materials showed significantly reduced inflammatory reactions (**Figure 6a**, iii–vi). The clinical scoring, using the criteria reported by Copland *et al.*,[28] showed that eyes from CTB-ACE2 or CTB-Ang-(1–7) fed animals had significantly improved clinical scores (EAU grade, 2.3 ± 1.2 and 2.3 ± 1.3 respectively) compared to eyes from animals fed with WT leaf (EAU grade, 3.4 ± 0.53) (**Figure 6b**).

The uveoretinitis was also evaluated by OCT imaging on day 14 after immunization with IRBP. In few cases, severe retinal pathology such as high level of cellular infiltration, edema, folds, and hemorrhages limited OCT resolution of retinal layers. In most cases, intravitreal cellular infiltration, retinal vasculitis, disorganized retinal layers and increased retinal thickness due to retinal folds and edema, can be easily visualized with OCT imaging as shown in **Figure 7a** in untreated or WT leaf material treated animals, these pathologies are much improved in mice treated with CTB-ACE2 or Ang-(1–7) (**Figure 7a**). Treatment with CTB-ACE2 or CTB-Ang-(1–7) leaf materials significantly reduced EAU-induced increased retinal thickness (269 ± 32 μm and 241 ± 52 μm respectively) compared to eyes treated with WT leaf (316 ± 32 μm) (**Figure 7b**).

Oral administration of CTB-ACE2 and CTB-Ang-(1–7) ameliorates histological findings in the EAU mice

Histological examination on day 14 showed a severe intraocular inflammation evidenced by massive infiltration of inflammatory cells, intensive retinal vasculitits, and changes in the retinal thickness, folding of retina, as well as photoreceptor damage in the WT leaf fed mice (**Figure 8a**). However, only scattered inflammation of inflammatory cells and minor retinal folding was observed in CTB-ACE2 or CTB-Ang-(1–7) treated animals (**Figure 8a**). Histopathological grading, using the criteria reported by Thurau *et al.*[29] showed that WT leaf fed eyes (EAU grade, 2.95 ± 0.717) had significantly severe inflammation as compared to CTB-ACE2

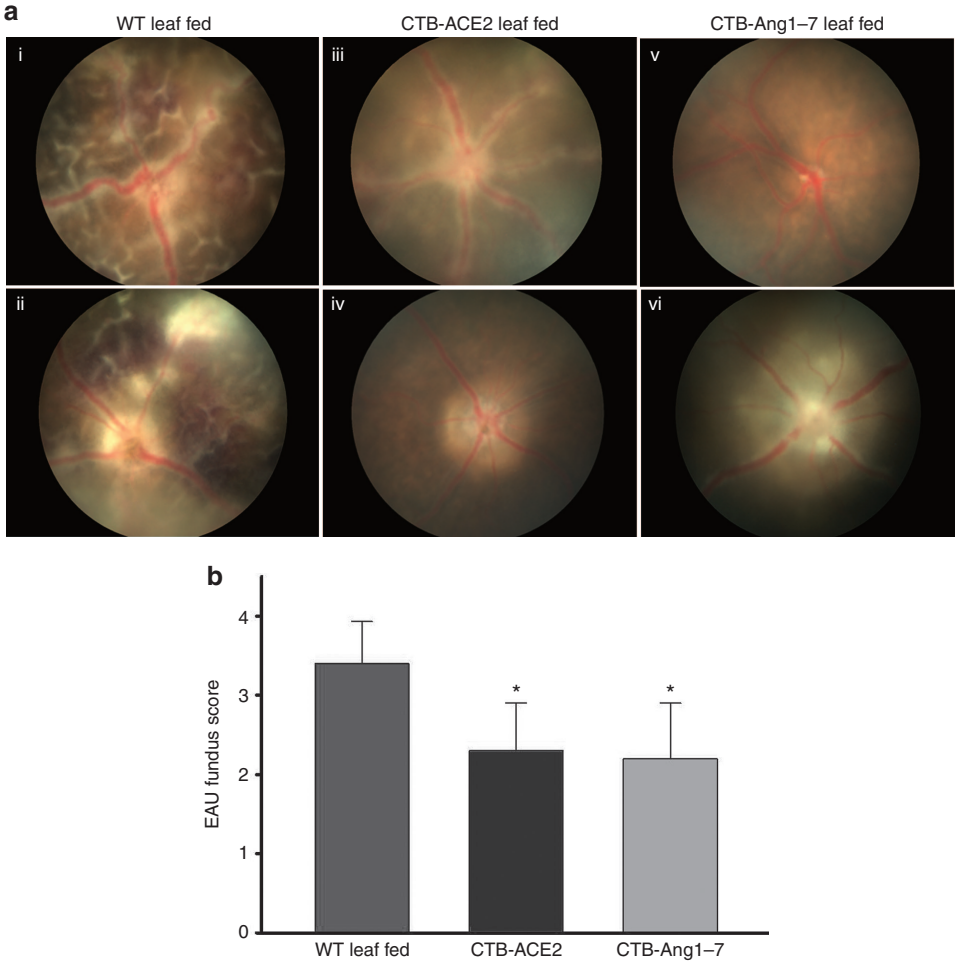

Figure 6 Clinical evaluation of EAU from fundoscopic photographs. EAU was induced in B10.RIII mice by immunization with IRBP in CFA. The fundoscopic images were obtained on day 14 after immunization. (**a**) Representative fundus image from (i,ii) WT leaf fed mice; (iii,iv) CTB-ACE2 expressed leaf fed mice; and (v,vi) CTB-Ang-(1–7) expressed leaf fed mice. (**b**) Clinical EAU scores. Clinical EAU score was evaluated on a scale of 0–4. Values on y-axis represent the average of clinical scores given on fundus images. Results are given as mean + SD; (n = 5 per group); *P < 0.05 (versus WT fed group).

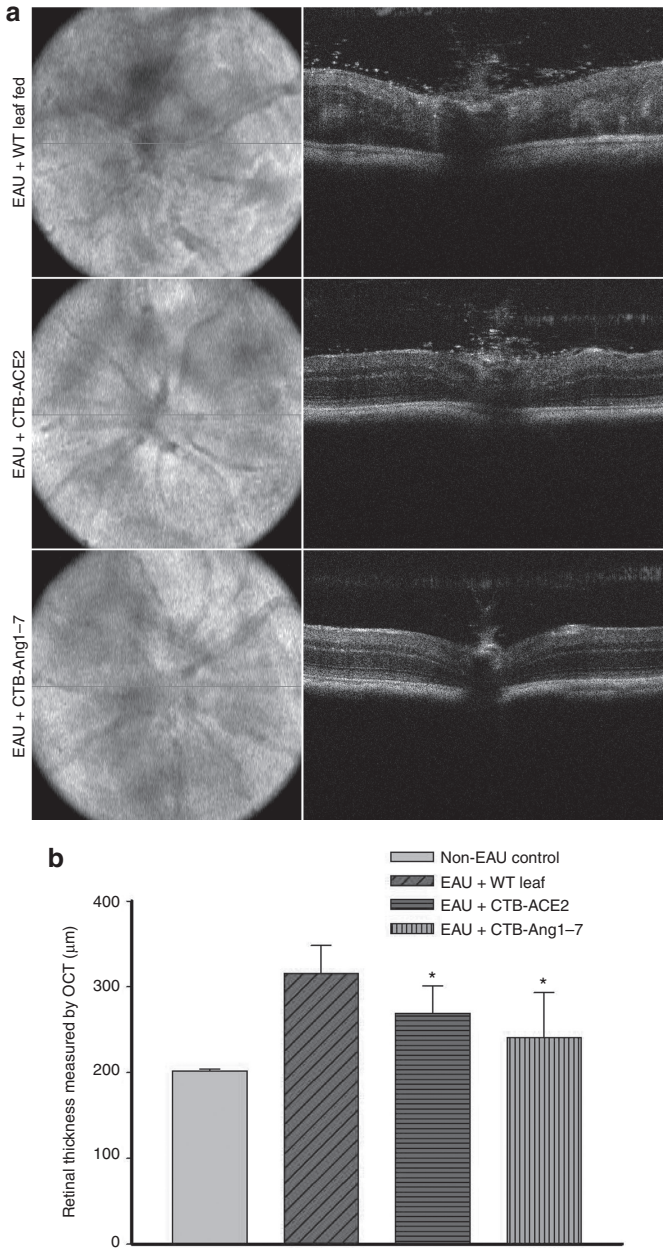

Figure 7 Assessment of retinal thickness on OCT images from EAU mice. Horizontal and cross sectional OCT images were obtained on day 14 after immunization. The retinal thickness was measured and averaged from five different frames of horizontal OCT scan images of single eye. (**a**) Representative fundus projection (left panel) and B-scan (right panel) images from WT leaf fed mice; CTB-ACE2 expressed leaf fed mice; and CTB-Ang-(1–7) expressed leaf fed mice. (**b**) Retinal thickness measured from OCT images. Values on y-axis represent the average of retinal thickness calculated manually from B-scan OCT images. Results are given as mean + SD; (n = 5 per group); *P < 0.05 (versus WT fed group).

(EAU grade, 1.1 ± 0.616) and CTB-Ang-(1–7) (EAU grade, 0.92 ± 0.535) expressed leaf fed eyes (**Figure 8b**). Similarly, significantly higher numbers of inflammatory cells were observed in the posterior chamber of WT leaf fed mice compared to the CTB-ACE2/Ang-(1–7) expressed leaf fed mice (**Figure 8b**).

To determine whether CTB-Ang-(1–7) treatment can also improve EAU after its onset or during its progression, daily oral feeding was delayed to day 5 and day 10 after EAU induction, and continued to day 14 when mice were euthanized for evaluation (**Supplementary Materials and Methods**). We observed that feeding from day 5 onward up to day 14 after IRBP injection is equally as effective as feeding from day 0, but feeding started at 10 after EAU induction had no improvement of ocular pathology (**Supplementary Figure S2**).

DISCUSSION

In this study, we have developed an expression system to generate high levels of human ACE2 and Ang-(1–7) within plant chloroplasts using transplastomic technology. Oral gavage of plant cells expressing ACE2 and Ang-(1–7) fused with CTB in mice resulted in increased circulating and retinal levels of ACE2 and Ang-(1–7), reduced ocular inflammation in two different models: endotoxin-induced uveitis (EIU) and autoantigen induced experimental autoimmune uveoretinitis (EAU).

Among many advantages of transplastomic technology, the high copy number of a transgene, up to >10,000 copies per cell, is a key to successful high level production of therapeutic proteins in chloroplasts. However, this advantage could be limited when human transgenes are not codon-optimized because the preference of codon usage of chloroplast is different from that of eukaryotic cell. The codon adjustment for chloroplast expression system is crucial for the efficient expression of human genes.[30] So, the relatively low expression ACE2 over the Ang-(1–7) is probably due to the use of native human gene sequence (805 amino acids). However, several other tools were incorporated into our system to offset low expression of the transgenes so that the contents of therapeutic proteins expressed in chloroplasts can be increased. For example, the expression of therapeutic proteins under the control of light-regulated strong chloroplast promoter, harvest of mature leaves at the end of day, and lyophilization of the harvested leaves. The chloroplast *psbA* promoter is light regulated and therefore harvesting leaves expressing therapeutic proteins before sunset maximizes the accumulation of therapeutic proteins. Moreover, the amount of therapeutic proteins in plant leaves can be concentrated by lyophilization (**Figure 2c**,**d**). The lyophilized therapeutic leaves need to be powdered and capsulized in clinical use for oral delivery and long-term storage. The process of dehydration of the leaves under vacuum at −51 °C for 3 days can significantly reduce the risk of microbial contamination.[11] The long-term shelf life of the lyophilized proteins at room temperature, up to 15 months,[11] can also decrease the cost associated with the cold chain of current injectable proteins.[11] The effect of lyophilization on the stability of proteins expressed in chloroplasts has been extensively studied in our lab under the condition at which temperature and pressure were set up at −51 °C and 27 mTorr, respectively, according to the chart of vapor pressure of ice provided by manufacturer. When the effect of duration of lyophilization was investigated, large protective antigen (PA, 83 kDa) expressed in lettuce chloroplasts was stable at 24, 48, and 72 hours of lyophilization. In addition, the lyophilized antigen was more stable at room temperature than the commercially purified antigens stored at low temperatures. Furthermore, the lyophilized PA was found to be stable up to 15 months at room temperature without any degradation.[11] Other transplastomic plants expressing CTB-exendin 4 (ref. [18]) and CTB-Factor VIII[31]

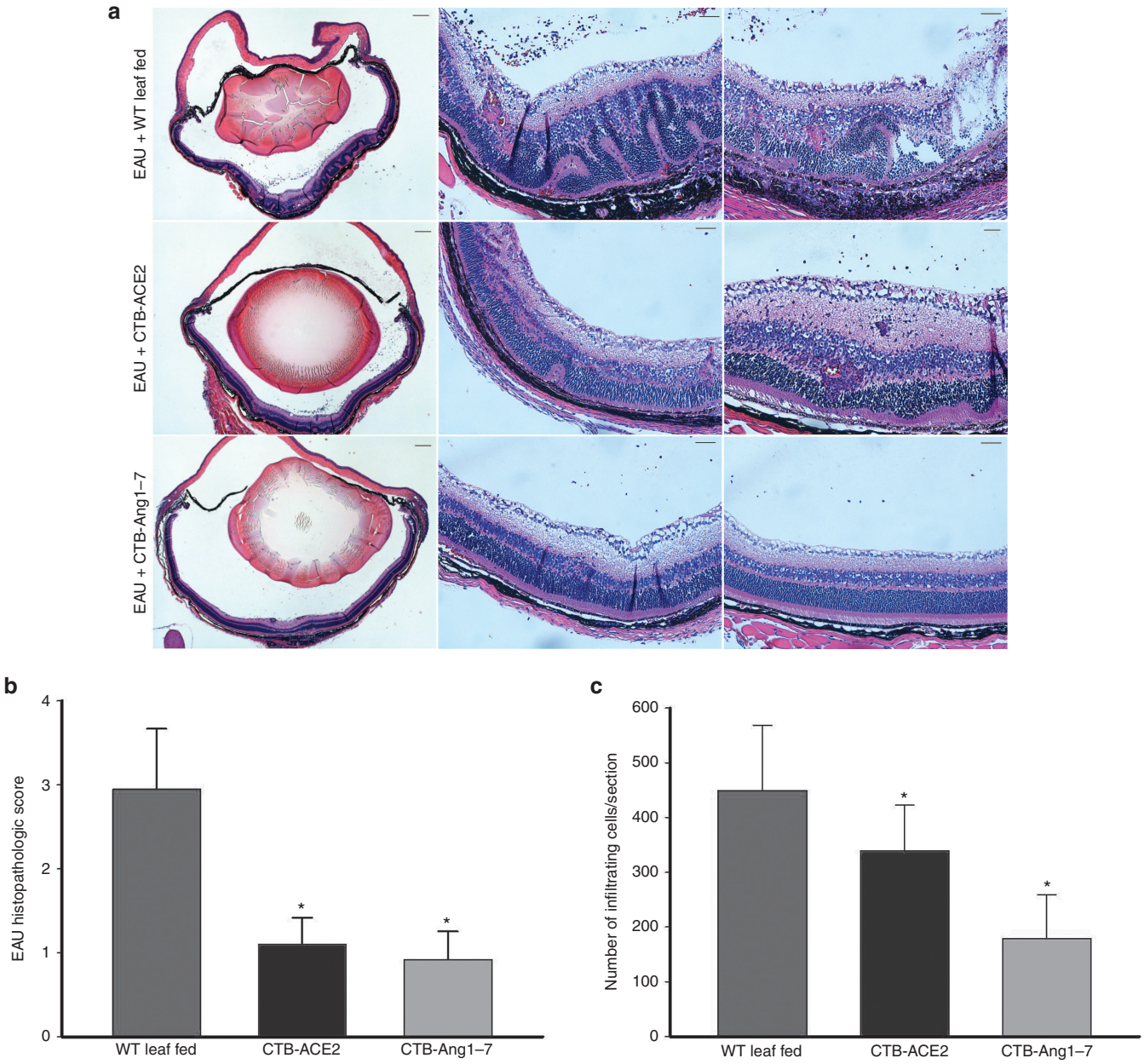

Figure 8 Histological evaluation of EAU. (**a**) Representative micrographs from animals fed with WT leaf fed mice, CTB-ACE2, and CTB-Ang-(1–7) leaf materials. Left panel: magnifications 40×, scale bar = 200 µm; right panels: 200×, scale bar = 50 µm. Images of histological analysis show severe retinal folding, loss of the photoreceptor layer and massive inflammatory cell inflammation in the vitreous, retina and subretinal space in WT leaf fed group; moderate to minimum infiltration, photoreceptor damage, retinal folding was observed in CTB-ACE2 expressed leaf fed group; a minor infiltration of cells and retinal folding was observed in the CTB-Ang-(1–7) leaf fed group. (**b**) Histopathology scores. CTB-ACE2 and CTB-Ang-(1–7) leaf fed groups showed a reduced EAU histological grade compared to controls fed with WT leaf. (**c**) Evaluation of infiltrating inflammatory cells in the posterior chamber. Inflammatory cells/section in the posterior chamber were counted on 14th day after EAU induction. Values on y-axis represent no. of infiltrating inflammatory cells/section. Results are given as mean + SD; (n = 5 per group); *P < 0.05 (versus WT leaf fed group).

showed similar stability of fusion proteins and protection of their assembly, folding and disulfide bonds similar to fresh leaves.

Drug delivery to different compartments of the eye, particularly to the posterior segment of the eye, is a major challenge due to several barriers formed by both anatomical structure and the protective physiological mechanisms of the eye.[10] Large molecular weight therapeutics such as peptides/proteins and oligonucleotides are delivered mostly via intravitreal route. However, frequent administration via this route is often associated with many complications such as retinal detachment, endophthalmitis, and increased intraocular pressure.[32,33] We demonstrate that oral administration of CTB-ACE2 increased ACE2 activity in sera and retina. Similarly increased level of plasma and retinal Ang-(1–7) was observed when the animals were orally administered with CTB-Ang-(1–7), as observed in previous study of oral delivery of bioencapsulated proteins across blood-brain and retinal barriers.[23] The increased level of the Ang-(1–7) could be stemmed from the fusion with CTB. The short peptide of Ang-(1–7) fused to CTB becomes stabilized in a

form of pentameric structure in plant cells (**Figure 2a**). However, only monomers are observed in sera once delivered into circulation. Considering that the efficiency of furin cleavage site depends on the flanking amino acid sequence of the fused protein,[34] Ang-(1–7) fusion to CTB did not offer optimal furin cleavage site. Thus, the cleavage between CTB and Ang-(1–7) is not likely to be fast or efficient once the fusion protein gets into sera. In addition, the CTB fusion provides N-terminal protection for Ang-(1–7) so its stability is extended for several hours, while injectable Ang-(1–7) has a very short half-life in sera.[35,36] Although the Ang-(1–7) level was increased in both plasma and retina (**Figure 3d**), the level of Ang-(1–7) increase in plasma was less than in retina (**Figure 3d**). This difference could be attributed to the increased retention in tissues (cells) and to their rapid clearance in the sera by proteases. Similar result was also observed in our previously published study in which GFP level was shown several fold higher in tissues than in sera.[23]

Although EIU was originally used as a model of anterior uveitis because of its characteristic infiltration of leucocytes into the anterior chamber of the eye,[4] growing evidences suggest that it also involves inflammation in the posterior segment of the eye, with recruitment of leucocytes that adhere to the retinal vasculature and infiltrate the vitreous cavity.[3] Our results demonstrate that enhanced level of ACE2/Ang-(1–7) in both circulation and ocular tissues suppressed the endotoxin-induced ocular inflammation, which is evident from significantly reduced number of infiltrating inflammatory cells in the iris-ciliary body, anterior and posterior chambers. This result is consistent with studies showing anti-inflammatory property of ACE2/Ang-(1–7) in other disease models.[7] The dose dependent study using bio-encapsulated lyophilized CTB-ACE2 in EIU model further confirmed that a dose of ~50 mg/day for four days can significantly prevent the endotoxin-induced inflammation. We also showed that increased ACE2/Ang-(1–7) significantly suppressed the LPS-induced ocular expression of IL-6, IL-1β, TNF-α, and VEGF. It has been reported that in EIU model, leucocytes are markedly attracted to inflamed ocular tissues such as the iris,[37] vitreous cavity[38] and retina,[39] with neutrophils and macrophages being major leucocyte constituents. MCP-1 is known as one of the important factors for leucocyte recruitment, and is up-regulated during EIU[40] whereas ICAM-1 is known to be the key molecule of leucocyte adhesion and/or transmigration.[41] Our study demonstrates that mice fed with ACE2/Ang-(1–7) leaf materials showed decreased ocular expression of MCP-1 and ICAM-1 in EIU eyes, contributing to the diminished inflammatory response by inhibiting leucocyte recruitment and adhesion in the ocular tissue. These results are consistent with the histopathology observation that LPS-induced acute inflammation caused the increase of inflammatory cell recruitment, while ACE2/Ang-(1–7) treatment significantly reduced the inflammatory cells in iris/ciliary body, anterior and posterior chamber.

It has been shown that ACE2/Ang-(1–7) may directly reduce inflammatory responses in immune cells such as macrophages.[42] Our study also shows modulatory ability of ACE2/Ang-(1–7) on local immune response and cytokine/chemokine expression. In fact, the Mas receptor is expressed not only in retinal vascular cells, astrocytes and muller glia, but also in retinal neurons, consistent with its role in neuro-vascular and immune response modulation. Moreover, our results show that eyes with EIU are associated with decreased expression of ACE2 and Mas receptor and increased expression of vasoconstrictive axis genes such as ACE, AT1Ra, AT1Rb during EIU. This is prevented by ACE2/Ang (1–7), suggesting that the anti-inflammatory effect of ACE2/Ang-(1–7) may be associated with Mas receptor and ACE2 up-regulation, and down-regulation of ACE and AT1Ra/AT1Rb, resulting in reduction of ocular inflammation.

In this study, we also investigated the effect of oral administration of CTB-ACE2/Ang-(1–7) on the development of EAU in mice and showed significant improvement of EAU eyes in mice treated with CTB-ACE2/Ang-(1–7). The pathogenesis of EAU is different from EIU. EAU is defined primarily as posterior segment disease as the target antigens reside in the retina and characterized by cellular infiltrates, retinal folds, detachment, granulomatous infiltrates in the retina and choroid, vasculitis, retinal neovascularization, mild to severe photoreceptor loss.[29] Histopathological examination confirmed a significant overall reduction of disease severity in the CTB-ACE2/Ang-(1–7) treatment groups evaluated by non-invasive funduscopy and OCT imaging methods. Furthermore, the retinal detachment, photoreceptor layer damage, infiltration of inflammatory cells was markedly prevented by CTB-ACE2/Ang-(1–7) treatments. Some of the fundoscopically normal-looking eyes showed few foci of very mild cellular infiltrates on histological evaluation. This is consistent with the findings from OCT imaging, demonstrating a better correlation of histological findings and pathological changes revealed by non-invasive OCT imaging in the retina during EAU. Thus, oral administration of CTB-ACE2/Ang-(1–7) from the induction to peak of EAU was able to ameliorate the progression of disease evaluated by clinical funduscopic score, OCT imaging and histopathological observation. Moreover, delayed oral administration of CTB-ACE2/Ang-(1–7) from day 5 after EAU induction was also able to decrease the progression of EAU.

Increasing evidence has shown that shifting the balance of RAS towards the protective axis by activation of ACE2 or its product, Ang-(1–7) is beneficial and anti-inflammatory.[7,43] Our findings also demonstrate that oral administration of CTB-ACE2/Ang-(1–7) provides robust protective anti-inflammatory effects against the pathophysiology in both EIU and EAU models. Nevertheless, future studies to further elucidate the molecular and cellular mechanisms underlying the anti-inflammatory effects of Ang-(1–7) and ACE2, to further define the pharmacokinetics and potential impact on other tissues/organs following oral administration will be essential for clinical applications. The recombinant CTB has already been approved for human use a decade ago and is used by hundreds of millions of people around the globe.[44] There are several studies using CTB to induce immune tolerance by orally administered human proteins conjugated to CTB, which would be an added advantage for prolonged use of this protein for treatment. For instance, the symptoms of autoimmune diseases including diabetes,[16] arthritis,[45] uveitis,[46] and hemophilia[19,31] have been shown to be prevented or delayed. The successful induction of oral tolerance by CTB-autoantigen conjugates in experimental systems has been also proven in pilot clinical trials;[47] CTB-BD peptide treatment blocked relapse of uveitis and recurrence of uveitis for 10–18 months after cessation of treatment.[47] Therefore, we anticipate development of human ACE2 and Ang-(1–7) fused form to CTB would progress smoothly.

In conclusion, this study provides proof-of-concept for production of therapeutically active ACE2/Ang-(1–7) bioencapsulated in plant cells for cost effective oral therapy for ocular applications and enhancing ACE2/Ang-(1–7) using this approach may provide a new avenue and a novel therapeutic strategy for the treatment of acute uveitis, autoimmune uveoretinitis and other ocular diseases.

MATERIALS AND METHODS

Chloroplast transformation vector construction and regeneration of transplastomic lines. The cDNA for *ACE2* (accession: NM_021804) was used as the template to clone *CTB-ACE2* fusion gene into the intermediate vector. To clone *CTB-Ang-(1–7)* fusion gene, *CTB*-containing vector was used as template with a forward primer specific to *CTB* and a reverse primer specific to *CTB* but including nucleotide sequence corresponding to 7 amino acid of Ang-(1–7) peptide. The sequence-confirmed chimeric gene was cloned into chloroplast transformation vector, pLD. Delivery of the fusion genes into chloroplast genome, regeneration of transplastomic plants, and PCR analysis of the specific integration of the transgene were carried out according to the previously published methods.[48]

Western blot analysis and quantification. Western blot and densitometric analysis were performed for the quantification of CTB-Ang-(1–7). Total leaf protein and purified CTB standard protein (Sigma-Aldrich, St Louis, MO) were separated on SDS-polyacrylamide gel and transferred to nitrocellulose membranes. Rabbit anti-CTB polyclonal antibody (GenWay Biotech, San Diego, CA) was used to probe the fusion proteins and then the developed films were scanned for quantitative analysis using Image J (IJ 1.46r; NIH) software. Standard curve was created using the known amounts of CTB standard and then the protein samples were interpolated on the graph.

ELISA was performed to quantify CTB-ACE2 protein. Serially diluted CTB and CTB-ACE2 in bicarbonate buffer were used for coating 96-well plates. The rabbit anti-CTB polyclonal antibody and goat anti-rabbit IgG-HRP antibody (Southern Biotechnology, Birmingham, AL) was used for immunodetection. Tetramethylbenzidine (TMB) was used as substrate (American Qualex Antibodies, San Clemente, CA) for the peroxidase and the color change was read spectrophotometrically at a wavelength of 450 nm.

For *in vivo* protein sample analysis, western blotting was performed with rabbit anti-CTB (Abcam, Cambridge, MA) and rabbit anti-ACE2 (Santa Cruz Biotechnology, Dallas, TX), and mouse β-actin antibodies (Sigma-Aldrich) and bound antibody detected using Odyssey imaging system (Li-Cor, Lincoln, NE).

CTB-GM1 binding assay. The formation of pentameric structure of CTB fused therapeutic proteins expressed in chloroplasts was investigated using CTB-GM1 ELISA method described earlier.[23] Monosialoganglioside-GM1 (Sigma-Aldrich, G-7641) coated ninety-six-well plates were incubated with homogenate plant proteins, which were serially diluted up to 10 pg/μl, at 4 °C, along with purified CTB and untransformed WT plant protein (10 ng/μl) as positive and negative control, respectively. After washing the plates thrice with 1X phosphate buffered saline with 0.05% (v/v) Tween-20 (PBST), the plate was blocked with 1X PBST (0.05% Tween 20) with 3% non-fat dry milk (PTM) for 1 hour at 37 °C. To detect the interaction between CTB pentamer and GM1, anti-CTB antibody (1:10,000 in PTM; GenWay Biotech) and IgG-HRP secondary antibody (1:4,000 in PTM; Southern Biotechnology) were used. The binding affinity was quantitatively analyzed as a function of absorbance at 450 nm using plate reader (Bio-Rad Life Sciences, Hercules, CA, Model 680) after incubation with 100 μl of tetramethylbenzidine (TMB) solution substrate (American Qualex Antibodies, San Clemente, CA). An absorbance of ≥ 0.1 after background signal substraction was determined as positive.

Lyophilization. The harvested leaves from greenhouse were rinsed with water then frozen in liquid nitrogen, and crumbled into small pieces. For freeze-drying, containers were sealed with porous 3M Millipore Medical Tape and then lyophilized in VirtisBenchtop Freeze Dry Systems (SP Scientific, Gardiner, NY) Lyophilized leaf material was ground into fine powers using ordinary coffee grinder and stored in sealed container at room temperature with silica gel until use.

Animals and experimental procedures. WT C57Bl/6J mice (6–8 weeks old) and B10.RIII mice (8–10 weeks old) were purchased from Jackson Laboratories (Bar Harbor, ME) and maintained at the Animal Care Service at the University of Florida. All procedures adhered to the ARVO statement for the use of Animals in Ophthalmic and Vision Research, and the protocol was approved by the Animal Care and Use Committee of the University of Florida. The animals were fed standard laboratory chow and allowed free access to water in an air-conditioned room with a 12–12-hours light–dark cycle.

The mice were divided in three groups for EIU model and orally gavaged with control (untransformed WT) tobacco leaves, CTB-ACE2, and CTB-Ang-(1–7) expressing transplastomic tobacco leaves. The mice were given ~500 mg of the specified tobacco leaf material suspended in sterile PBS, by careful gavage into the hypopharynx twice in a day for 5 days. For preparation of the gavage material, leaves were frozen and ground in liquid nitrogen. EIU was induced by a single intravitreal injection of *Escherichia coli* LPS (25 ng/eye) (Sigma-Aldrich) dissolved in sterile pyrogen-free saline, on the fifth day of feeding. All animals were anesthetized and pupils were dilated before intraocular injections. Each experimental group included at least 4–6 animals and each experiment was performed at least twice.

For the EAU model, the mice were divided in three groups and orally gavaged with ~500 mg of the control WT tobacco leaves, CTB-ACE2, CTB-Ang-(1–7) expressing transplastomic tobacco leaves once daily for 15 days. EAU was induced by active immunization with ~50 μg of IRBP (161–180) (SGIPYIISYLHPGNTILHVD) (Genscript, Piscataway, NJ) with CFA (Sigma-Aldrich) (1:1 vol/vol) subcutaneously, on the second day of feeding. Each experimental group included at least four to six animals and each experiment was performed at least twice to ensure reproducibility.

Histopathological evaluation. The EIU mice were euthanized 24 hours after LPS injection and the eyes were enucleated immediately and fixed in 4% paraformaldehyde freshly made in PBS overnight at 4 °C and processed for paraffin embedding and sections. Sagittal sections (4 μm) from every 50 μm were cut and stained with hematoxylin and eosin (H&E). The anterior and posterior chambers were examined under light microscope and the infiltrating inflammatory cells were counted in a masked fashion. The number of infiltrating inflammatory cells in five sections per eye was averaged and recorded. EIU clinical data shown were representatives of three sets of experiments.

The EAU mice were euthanized and the eyes were harvested on 14th day after immunization, followed by fixation, paraffin embedment and stained with H&E. The severity of EAU was evaluated in a masked fashion on a scale of 0–4 using previously published criteria based on the number, type and size of lesions[29] and the inflammatory cells were counted as described above. EAU clinical data shown were representatives of two sets of experiments, five animals each experimental group.

ACE2 activity assay. Representative retinas from each group of mice were dissected and homogenized by sonication in ACE2 assay buffer. The ACE2 activity assay was performed using 100 μg of retinal protein in black 96-well opaque plates with 50 μmol/l ACE2-specific fluorogenic peptide substrate VI (R&D Systems, Minneapolis, MN) in a final volume of 100 μl per well reaction mixture. The enzymatic activity was recorded in a SpectraMax M3 fluorescence microplate reader (Molecular Devices, LLC, Sunnyvale, CA) for 2 hours with excitation at 340 nm and emission at 400 nm as described previously.[8] For the sera samples, 10 μl sera were used in a 100 μl reaction. All measurements were performed in duplicate and the data represent the mean of three assay results.

Table 1 Primers used for real-time RT-PCR analysis

Gene name	Accession number	Sequences
Interleukin-6	NM_031168.1	Forward: 5'-TCGGCAAACCTAGTGCGTTA -3'
		Reverse: 5'-CCAAGAAACCATCTGGCTAGG-3'
IL-1β	NM_008361.3	Forward: 5'-AAAGCCTCGTGCTGTCGGACC -3'
		Reverse: 5'-CAGCTGCAGGGTGGGTGTGC -3'
TNF-α	NM_013693.2	Forward: 5'-AGGCGCCACATCTCCCTCCA-3'
		Reverse: 5'-CGGTGTGGGTGAGGAGCACG-3'
ICAM-1	NM_010493	Forward: 5'-AGATGACCTGCAGACGGAAG-3'
		Reverse: 5'-GGCTGAGGGTAAATGCTGTC-3'
MCP-1	NM_011333	Forward: 5'-CCCCACTCACCTGCTGCTACT-3'
		Reverse: 5'-GGCATCACAGTCCGAGTCACA-3'
β-Actin	X03672	Forward: 5'-AGCAGATGTGGATCAGCAAG-3'
		Reverse: 5'-ACAGAAGCAATGCTGTCACC-3'
MAS receptor	NM_008552	Forward: 5′-AGGGTGACTGACTGAGTTTGG-3′
		Reverse: 5′-GAAGGTAAGAGGACAGGAGC-3′
AT1Ra	NM_177322	Forward: 5'-ATCGGACTAAATGGCTCACG-3'
		Reverse: 5'-ACGTGGGTCTCCATTGCTAA-3'
AT1Rb	AK087228	Forward: 5'-AGTGGAGTGAGAGGGTTCAA-3'
		Reverse: 5'-GGGCATTGAAGACATGGTAT-3'

Ang-(1–7) estimation by enzyme immunoassay. The level of Ang-(1–7) in plasma and retina were measured using a commercial EIA kit (Bachem, San Carlos, CA), according to the manufacturer's instructions. All measurements were performed in duplicate and the data represent the mean of two separate assay results.

Real time RT-PCR analysis. Total RNA was isolated from freshly enucleated eyes using Trizol Reagent (Invitrogen, Carlsbad, CA) according to manufacturer's instructions. Reverse transcription was performed using Enhanced Avian HS RT-PCR kit (Sigma-Aldrich) following manufacturer's instructions. Real time PCR was carried out on real time thermal cycler (iCycler, Bio-Rad Life Sciences) using iQTMSybr Green Supermix (Bio-Rad Life Sciences). The threshold cycle number (Ct) for real-time PCR was set by the cycler software. Optimal primer concentration for PCR was determined separately for each primer pair. Each reaction was run in duplicate or in triplicate, and reaction tubes with target primers and those with Actin primers were always included in the same PCR run. To test the primer efficiencies, the one-step reverse-transcriptase-PCR was run with each target primer. Relative quantification was achieved by the comparative $2^{-\Delta\Delta Ct}$ method 1. The relative increase/decrease of mRNA target X in the experimental group (EG) was calculated using the control group as the calibrator: $2^{-\Delta\Delta Ct}$, where ΔΔ Ct is {Ct. × [EG] – Ct. Actin [EG]} – {Ct. × [control] – Ct. Actin [control]}. Primer sequences used in this study are shown in **Table 1**. All the reactions were repeated at least twice.

Fundus imaging and assessment of EAU. Fundus assessment of EAU was performed at day 14 after EAU induction. The pupils were dilated using atropine sulfate and phenylephrine hydrochloride. The mice were anesthetized by intraperitoneal injection of ketamine (75 mg/kg) and xylazine (5 mg/kg) mixture, and GonakHypromellose demulcent ophthalmic solution (Akorn, Buffalo Grove, IL) was used on ocular surface. The fundus was imaged using the Micron II small animal retinal imaging AD camera (Phoenix Research Laboratories, Pleasanton, CA). Eyes were examined for vasculitis, focal lesions, linear lesions, retinal hemorrhages and retinal detachment. Clinical EAU scoring was performed on a scale of 0–4, as described in detail previously.[28] EAU clinical data shown was representative of two sets of experiments.

Spectral Domain Optical Coherence Tomography imaging and assessment of EAU mice. Mice were anesthetized and the pupil dilated as described above. Artificial tears (Systane Ultra, Alcon, Fort Worth, TX) were used throughout the procedure to maintain corneal moisture and clarity. Spectral Domain Optical Coherence Tomography (SD-OCT) images were obtained in mice on 14th day after immunization using the Bioptigen Spectral Domain Ophthalmic Imaging System (Bioptigen, Durham, NC). Images acquired by the software provided from the company. The average single B scan and volume scans were obtained with images centered on optic nerve head. The retinal thickness was measured from five frames of the volume of OCT images and averaged from the intensity peak of boundary corresponding to the vitreo-retinal interface to the intensity peak corresponding to the retinal pigmented epithelium.[49] EAU clinical data shown was representative of two sets of experiments.

Statistical analysis. Data are expressed as the mean + SD of at least two independent experiments. Differences between mean values of multiple groups were analyzed by one-way analysis of variance with Dunnett's test for post hoc comparisons. A P value less than 0.05 was considered statistically significant.

SUPPLEMENTARY MATERIAL

Figure S1. Histological evaluation of EIU mice. The mice were orally administered with different doses of lyophilized plant cells expressing CTB-ACE2 for 4 days before LPS(25ng/eye)injection.

Figure S2. Evaluation of EAU from fundoscopic photographs, OCT and histopatholgy. EAU was induced in B10.RIII mice by immunization with IRBP in CFA.

Materials and Methods.

ACKNOWLEDGMENTS

We thank Dheeraj Verma in the Daniell lab for making chloroplast vectors. The authors declare no conflict of interest.

REFERENCES

1. Mochizuki, M, Sugita, S and Kamoi, K (2013). Immunological homeostasis of the eye. *Prog Retin Eye Res* **33**: 10–27.
2. Read, RW (2006). Uveitis: advances in understanding of pathogenesis and treatment. *Curr Rheumatol Rep* **8**: 260–266.
3. Rosenbaum, JT, McDevitt, HO, Guss, RB and Egbert, PR (1980). Endotoxin-induced uveitis in rats as a model for human disease. *Nature* **286**: 611–613.
4. Agarwal, RK, Silver, PB and Caspi, RR (2012). Rodent models of experimental autoimmune uveitis. *Methods Mol Biol* **900**: 443–469.
5. Paul, M, Poyan Mehr, A and Kreutz, R (2006). Physiology of local renin-angiotensin systems. *Physiol Rev* **86**: 747–803.
6. Santos, RA, Ferreira, AJ, Verano-Braga, T and Bader, M (2013). Angiotensin-converting enzyme 2, angiotensin-(1-7) and Mas: new players of the renin-angiotensin system. *J Endocrinol* **216**: R1–R17.
7. Simões e Silva, AC, Silveira, KD, Ferreira, AJ and Teixeira, MM (2013). ACE2, angiotensin-(1-7) and Mas receptor axis in inflammation and fibrosis. *Br J Pharmacol* **169**: 477–492.

8. Verma, A, Shan, Z, Lei, B, Yuan, L, Liu, X, Nakagawa, T *et al.* (2012). ACE2 and Ang-(1-7) confer protection against development of diabetic retinopathy. *Mol Ther* **20**: 28–36.
9. Qiu, Y, Shil, PK, Zhu, P, Yang, H, Verma, A, Lei, B *et al.* (2014). Angiotensin-converting enzyme 2 (ACE2) activator diminazene aceturate ameliorates endotoxin-induced uveitis in mice. *Invest Ophthalmol Vis Sci* **55**: 3809–3818.
10. Rawas-Qalaji, M and Williams, CA (2012). Advances in ocular drug delivery. *Curr Eye Res* **37**: 345–356.
11. Kwon, KC, Verma, D, Singh, ND, Herzog, R and Daniell, H (2013). Oral delivery of human biopharmaceuticals, autoantigens and vaccine antigens bioencapsulated in plant cells. *Adv Drug Deliv Rev* **65**: 782–799.
12. Daniell, H, Singh, ND, Mason, H and Streatfield, SJ (2009). Plant-made vaccine antigens and biopharmaceuticals. *Trends Plant Sci* **14**: 669–679.
13. Flint, HJ, Bayer, EA, Rincon, MT, Lamed, R and White, BA (2008). Polysaccharide utilization by gut bacteria: potential for new insights from genomic analysis. *Nat Rev Microbiol* **6**: 121–131.
14. Flint, HJ, Scott, KP, Duncan, SH, Louis, P and Forano, E (2012). Microbial degradation of complex carbohydrates in the gut. *Gut Microbes* **3**: 289–306.
15. Limaye, A, Koya, V, Samsam, M and Daniell, H (2006). Receptor-mediated oral delivery of a bioencapsulated green fluorescent protein expressed in transgenic chloroplasts into the mouse circulatory system. *FASEB J* **20**: 959–961.
16. Ruhlman, T, Ahangari, R, Devine, A, Samsam, M and Daniell, H (2007). Expression of cholera toxin B-proinsulin fusion protein in lettuce and tobacco chloroplasts–oral administration protects against development of insulitis in non-obese diabetic mice. *Plant Biotechnol J* **5**: 495–510.
17. Davoodi-Semiromi, A, Schreiber, M, Nalapalli, S, Verma, D, Singh, ND, Banks, RK *et al.* (2010). Chloroplast-derived vaccine antigens confer dual immunity against cholera and malaria by oral or injectable delivery. *Plant Biotechnol J* **8**: 223–242.
18. Kwon, KC, Nityanandam, R, New, JS and Daniell, H (2013). Oral delivery of bioencapsulated exendin-4 expressed in chloroplasts lowers blood glucose level in mice and stimulates insulin secretion in beta-TC6 cells. *Plant Biotechnol J* **11**: 77–86.
19. Verma, D, Moghimi, B, LoDuca, PA, Singh, HD, Hoffman, BE, Herzog, RW *et al.* (2010). Oral delivery of bioencapsulated coagulation factor IX prevents inhibitor formation and fatal anaphylaxis in hemophilia B mice. *Proc Natl Acad Sci USA* **107**: 7101–7106.
20. Wilson, JP (1967). Surface area of the small intestine in man. *Gut* **8**: 618–621.
21. Holmgren, J, Lönnroth, I, Månsson, J and Svennerholm, L (1975). Interaction of cholera toxin and membrane GM1 ganglioside of small intestine. *Proc Natl Acad Sci USA* **72**: 2520–2524.
22. Hadjiconstantinou, M and Neff, NH (1998). GM1 ganglioside: *in vivo* and *in vitro* trophic actions on central neurotransmitter systems. *J Neurochem* **70**: 1335–1345.
23. Kohli, N, Westerveld, DR, Ayache, AC, Verma, A, Shil, P, Prasad, T *et al.* (2014). Oral delivery of bioencapsulated proteins across blood-brain and blood-retinal barriers. *Mol Ther* **22**: 535–546.
24. Thomas, G (2002). Furin at the cutting edge: from protein traffic to embryogenesis and disease. *Nat Rev Mol Cell Biol* **3**: 753–766.
25. Miyata, T, Oshiro, S, Harakuni, T, Taira, T, Matsuzaki, G and Arakawa, T (2012). Physicochemically stable cholera toxin B subunit pentamer created by peripheral molecular constraints imposed by de novo-introduced intersubunit disulfide crosslinks. *Vaccine* **30**: 4225–4232.
26. Fletcher, EL, Phipps, JA, Ward, MM, Vessey, KA and Wilkinson-Berka, JL (2010). The renin-angiotensin system in retinal health and disease: Its influence on neurons, glia and the vasculature. *Prog Retin Eye Res* **29**: 284–311.
27. Hankey, DJ, Lightman, SL and Baker, D (2001). Interphotoreceptor retinoid binding protein peptide-induced uveitis in B10.RIII mice: characterization of disease parameters and immunomodulation. *Exp Eye Res* **72**: 341–350.
28. Copland, DA, Wertheim, MS, Armitage, WJ, Nicholson, LB, Raveney, BJ and Dick, AD (2008). The clinical time-course of experimental autoimmune uveoretinitis using topical endoscopic fundal imaging with histologic and cellular infiltrate correlation. *Invest Ophthalmol Vis Sci* **49**: 5458–5465.
29. Thurau, SR, Chan, CC, Nussenblatt, RB and Caspi, RR (1997). Oral tolerance in a murine model of relapsing experimental autoimmune uveoretinitis (EAU): induction of protective tolerance in primed animals. *Clin Exp Immunol* **109**: 370–376.
30. Daniell, H, Ruiz, G, Denes, B, Sandberg, L and Langridge, W (2009). Optimization of codon composition and regulatory elements for expression of human insulin like growth factor-1 in transgenic chloroplasts and evaluation of structural identity and function. *BMC Biotechnol* **9**: 33.
31. Sherman, A, Su, J, Lin, S, Wang, X, Herzog, RW and Daniell, H (2014). Suppression of inhibitor formation against FVIII in a murine model of hemophilia A by oral delivery of antigens bioencapsulated in plant cells. *Blood* **124**: 1659–1668.
32. Peyman, GA, Lad, EM and Moshfeghi, DM (2009). Intravitreal injection of therapeutic agents. *Retina* **29**: 875–912.
33. Wu, H and Chen, TC (2009). The effects of intravitreal ophthalmic medications on intraocular pressure. *Semin Ophthalmol* **24**: 100–105.
34. Duckert, P, Brunak, S and Blom, N (2004). Prediction of proprotein convertase cleavage sites. *Protein Eng Des Sel* **17**: 107–112.
35. Iusuf, D, Henning, RH, van Gilst, WH and Roks, AJ (2008). Angiotensin-(1-7): pharmacological properties and pharmacotherapeutic perspectives. *Eur J Pharmacol* **585**: 303–312.
36. Mordwinkin, NM, Russell, JR, Burke, AS, Dizerega, GS, Louie, SG and Rodgers, KE (2012). Toxicological and toxicokinetic analysis of angiotensin (1-7) in two species. *J Pharm Sci* **101**: 373–380.
37. Planck, SR, Becker, MD, Crespo, S, Choi, D, Galster, K, Garman, KL *et al.* (2008). Characterizing extravascular neutrophil migration *in vivo* in the iris. *Inflammation* **31**: 105–111.
38. Noda, K, Miyahara, S, Nakazawa, T, Almulki, L, Nakao, S, Hisatomi, T *et al.* (2008). Inhibition of vascular adhesion protein-1 suppresses endotoxin-induced uveitis. *FASEB J* **22**: 1094–1103.
39. Miyahara, S, Kiryu, J, Miyamoto, K, Katsuta, H, Hirose, F, Tamura, H *et al.* (2004). *In vivo* three-dimensional evaluation of leukocyte behavior in retinal microcirculation of mice. *Invest Ophthalmol Vis Sci* **45**: 4197–4201.
40. Satofuka, S, Ichihara, A, Nagai, N, Yamashiro, K, Koto, T, Shinoda, H *et al.* (2006). Suppression of ocular inflammation in endotoxin-induced uveitis by inhibiting nonproteolytic activation of prorenin. *Invest Ophthalmol Vis Sci* **47**: 2686–2692.
41. Whitcup, SM, Hikita, N, Shirao, M, Miyasaka, M, Tamatani, T, Mochizuki, M *et al.* (1995). Monoclonal antibodies against CD54 (ICAM-1) and CD11a (LFA-1) prevent and inhibit endotoxin-induced uveitis. *Exp Eye Res* **60**: 597–601.
42. Souza, LL and Costa-Neto, CM (2012). Angiotensin-(1-7) decreases LPS-induced inflammatory response in macrophages. *J Cell Physiol* **227**: 2117–2122.
43. Passos-Silva, DG, Verano-Braga, T and Santos, RA (2013). Angiotensin-(1-7): beyond the cardio-renal actions. *Clin Sci* **124**: 443–456.
44. Hill, DR, Ford, L and Lalloo, DG (2006). Oral cholera vaccines: use in clinical practice. *Lancet Infect Dis* **6**: 361–373.
45. Kim, N, Cheng, KC, Kwon, SS, Mora, R, Barbieri, M and Yoo, TJ (2001). Oral administration of collagen conjugated with cholera toxin induces tolerance to type II collagen and suppresses chondritis in an animal model of autoimmune ear disease. *Ann Otol Rhinol Laryngol* **110**: 646–654.
46. Phipps, PA, Stanford, MR, Sun, JB, Xiao, BG, Holmgren, J, Shinnick, T *et al.* (2003). Prevention of mucosally induced uveitis with a HSP60-derived peptide linked to cholera toxin B subunit. *Eur J Immunol* **33**: 224–232.
47. Stanford, M, Whittall, T, Bergmeier, LA, Lindblad, M, Lundin, S, Shinnick, T *et al.* (2004). Oral tolerization with peptide 336-351 linked to cholera toxin B subunit in preventing relapses of uveitis in Behcet's disease. *Clin Exp Immunol* **137**: 201–208.
48. Verma, D, Samson, NP, Koya, V and Daniell, H (2008). A protocol for expression of foreign genes in chloroplasts. *Nat Protoc* **3**: 739–758.
49. Chen, J, Qian, H, Horai, R, Chan, CC and Caspi, RR (2013). Use of optical coherence tomography and electroretinography to evaluate retinal pathology in a mouse model of autoimmune uveitis. *PLoS ONE* **8**: e63904.